Molecular Therapy
Nucleic Acids
Original Article

Elucidation of the Hdac2/Sp1/*miR-204-5p*/*Bcl-2* axis as a modulator of cochlear apoptosis via *in vivo*/*in vitro* models of acute hearing loss

Lisheng Xie,[1,3] Qiongqiong Zhou,[3] Xiaorui Chen,[2] Xiaoping Du,[4] Zhibiao Liu,[1] Bing Fei,[1] Jie Hou,[1] Yanhong Dai,[1] and Wandong She[1,2]

[1]Department of Otolaryngology-Head and Neck Surgery, Nanjing Drum Tower Hospital, Clinical College of Nanjing Medical University, Nanjing 210008, China; [2]Nanjing Drum Tower Hospital, Nanjing University of Chinese Medicine, Nanjing 210008, China; [3]Department of Otolaryngology, Children's Hospital of Nanjing Medical University, Nanjing 210008, China; [4]Hough Ear Institute, Oklahoma City, OK 73112, USA

We previously reported that dysregulation of histone deacetylase 2 (Hdac2) was associated with the prognosis of sudden sensorineural hearing loss. However, the underlying molecular mechanisms are poorly understood. In the present study, we developed an acute hearing loss animal model in guinea pigs by infusing lipopolysaccharides (LPS) into the cochlea and measured the expression of Hdac2 in the sensory epithelium. We observed that the level of Hdac2 was significantly decreased in the LPS-infused cochleae. The levels of apoptosis-inhibition genes *Bcl-2* and Bcl-xl were also decreased in the cochlea and correlated positively with the levels of Hdac2. Caspase3 or TUNEL-positive spiral ganglion neurons, hair cells, and supporting cells were observed in the LPS-infused cochleae. These *in vivo* observations were recapitulated in cell culture experiments. Based on bioinformatics analysis, we found *miR-204-5p* was engaged in the regulation of Hdac2 on Bcl-2. Molecular mechanism experiments displayed that *miR-204-5p* could be regulated by Hdac2 through interacting with transcription factor Sp1. Taken together, these results indicated that the Hdac2/Sp1/*miR-204-5p*/*Bcl-2* regulatory axis mediated apoptosis in the cochlea, providing potential insights into the progression of acute hearing loss. To our knowledge, the study describes a miRNA-related mechanism for Hdac2-mediated regulation in the cochlea for the first time.

INTRODUCTION

Histone deacetylase 2 (Hdac2) is known as a transcription suppressor through regulating the histone acetylation levels. It has been reported as a biological participant in various human diseases.[1–4] Our previous studies have suggested that HDCA2 might be involved in the pathogenesis of sudden sensorineural hearing loss (SSNHL).[5–8] However, the underlying molecular mechanism of Hdac2 has not been elucidated. SSNHL is an acute hearing loss with etiology unknown. Other acute sensorineural hearing loss includes noise- and drug-induced hearing loss.[9] Similar pathologic mechanisms may be involved in these types of sensorineural hearing loss. For example, reactive oxygen species (ROS) are accumulated in the cochlea shortly after noise or ototoxic drug exposure and actively stimulate intracellular stress pathways that can lead to apoptotic and/or necrotic hair cell death.[10,11] Although there is no direct evidence of involvement of apoptosis in SSNHL, previous studies indicated that oxidative stress plays a role in its pathogenesis.[12,13]

Apoptosis also acts as a common pathologic cell death mechanism in age-related hearing loss and autoimmune inner ear diseases.[14–17] Apoptosis within the cochlear sensory hair cell population has been observed in animal models of SSNHL, otitis media after middle ear lipopolysaccharide (LPS) application, and *in vitro* models of inner ear ischemia.[18–20]

Recent studies indicate that microRNA-207 and -34a can increase apoptosis of cochlear hair cells, suggesting that microRNAs (miRNAs) may participate in apoptotic cascades in the inner ear.[21,22] miRNAs are a class of short RNA molecules (~21 nucleotides [nt]) with no protein-coding ability, which guide the post-transcriptional regulation of target genes.[23–30] miRNAs have been confirmed to mediate biological processes in diseases by binding to the 3′-UTR of target messenger RNAs (mRNAs) and subsequently causing either mRNA degradation or translational inhibition. In recent years, miRNAs have been reported as regulators in cochlear hair cell apoptosis,[31,32] which implies their potential role in acute hearing loss.

A link among HDACs, miRNAs, and apoptosis has been discovered in cancers.[33,34] *miR-204-5p* has been reported to be involved in the regulation of inflammation, oxidative stress, inhibition of tumor

Received 19 March 2020; accepted 14 January 2021;
https://doi.org/10.1016/j.omtn.2021.01.017.

Correspondence: Wandong She, Department of Otolaryngology-Head and Neck Surgery, Nanjing Drum Tower Hospital, Clinical College of Nanjing Medical University, 321 Zhongshan Road, Nanjing 210008, China.
E-mail: shewandong@163.com
Correspondence: Yanhong Dai, Department of Otolaryngology-Head and Neck Surgery, Nanjing Drum Tower Hospital, Clinical College of Nanjing Medical University: 321 Zhongshan Road, Nanjing 210008, China.
E-mail: daiyanhong9@126.com

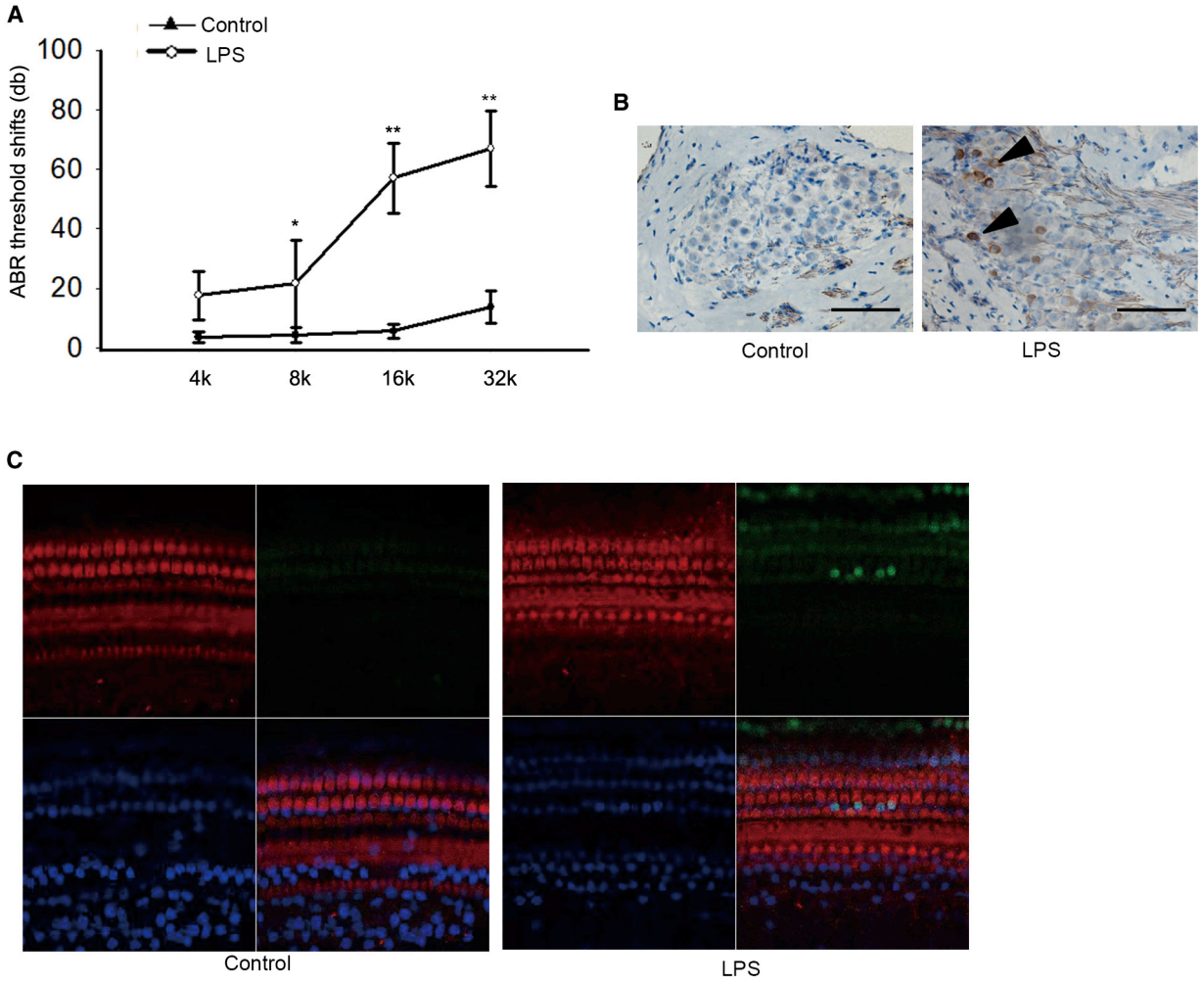

Figure 1. Hearing loss and apoptosis in guinea pig cochleae infused with LPS

(A) Guinea pigs infused with LPS exhibited significantly greater ABR threshold shifts than those in the artificial perilymph (AP)-infused control group (control) at 8, 16, and 32 kHz (*$p < 0.05$, **$p < 0.01$). (B) Caspase-3-positive cells were observed in the spiral ganglion of cochleae from the LPS infusion group (arrows in B), while no immunopositive cells were observed in the control group. (C) TUNEL-positive cochlear hair cell (arrow) and supporting cells (arrowheads) were observed in the LPS group, while no positive cells were observed in the control group (red: myosin 7a; green: apoptotic cells; blue: DAPI). Data in (A) are displayed as mean ± SD (three guinea pigs in each group).

growth, and metastasis.[35–38] However, *miR-204-5p* has not yet been described in hearing loss. Based on our previous studies with Hdac2, the involvement of apoptosis in acute hearing loss and the well-built connection of HDACs and *miR-204-5p* with apoptosis in cancer models, we hypothesized that Hdac2 activity might contribute to the regulation of cochlear hair cell apoptosis by miRNAs both in an animal model of acute hearing loss[5] and in HEI-OC1 cells *in vitro*. We observed that the level of Hdac2 was distinctly decreased in the cochlear cells treated with LPS, in concert with declined levels of the anti-apoptotic proteins *Bcl-2* and Bcl-xl. Sp1 is a transcription regulator known to participate in various biological processes.[39–42] Hdac2 and Sp1 can form a complex to regulate transcription.[43] The present study demonstrated that Sp1 was involved in the regulation of Hdac2 on *miR-204-5p*. Collectively, this study revealed a role of Hdac2/miR-204-5P/*Bcl-2* axis in the apoptosis of cochlear cells.

RESULTS

Hearing loss and apoptosis in guinea pigs treated with LPS

Consistent with our previous report,[5] significant hearing loss was observed in the LPS group compared to the control group. Averaged auditory brainstem response (ABR) threshold shifts were 17.5 ± 8.4, 21.6 ± 14.1, 58.3 ± 11.8, and 64.2 ± 12.7 dB at 4, 8, 16, and 32 kHz, respectively, in LPS-infused guinea pigs; averaged ABR threshold shifts were 3.8 ± 1.5, 4.9 ± 2.3, 6.7 ± 2.0, and 15.1 ± 4.6 dB in artificial perilymph (AP)-infused guinea pigs. As illustrated in Figure 1A, guinea pigs infused with LPS exhibited significantly greater ABR threshold shifts at 8, 16, and 32 kHz compared to the control group

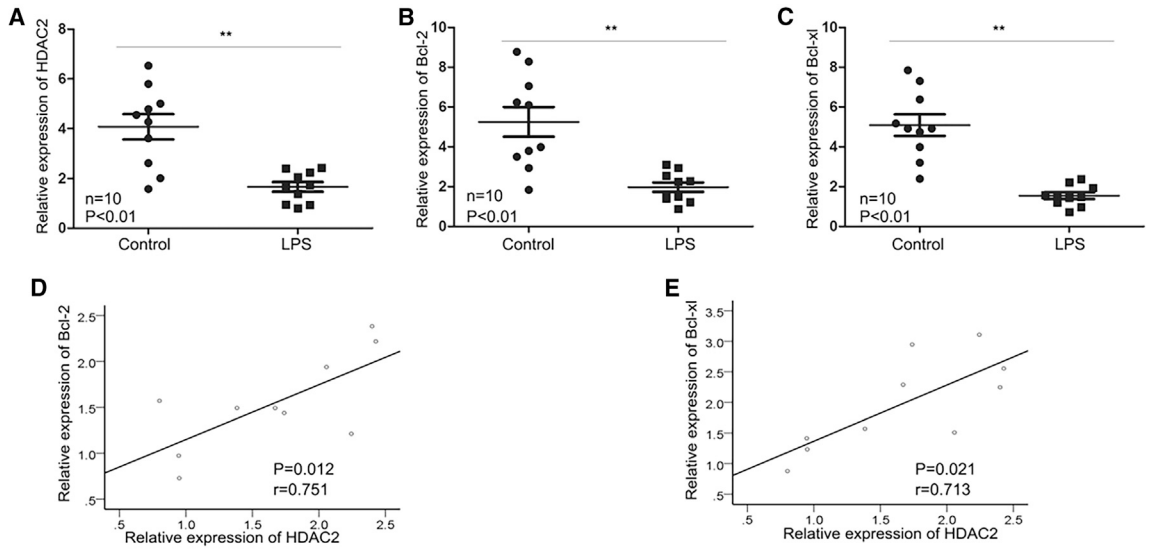

Figure 2. Decreased mRNA expression levels of HDAC2 and apoptosis-related genes (Bcl-2 and Bcl-xL) in LPS-infused cochleae

(A–C) The mRNA expression of HDAC2, Bcl-2, or Bcl-xL in the control (AP) and LPS-infused cochleae were determined by qRT-PCR. LPS treatment significantly decreased the expression of HDAC2 (A), Bcl-2 (B), and Bcl-xL (C) in the cochleae compared to the control group (**p < 0.01 in A–C). (D and E) Pearson correlation analysis demonstrated a positive correlation between the levels of HDAC2 and anti-apoptotic genes: Bcl-2 (D) and Bcl-xL (E). All data displayed as mean ± SD were obtained from three repeated and independent assays.

(unpaired Student's t test, *p < 0.05, **p < 0.01, n = 16), indicating that LPS induced a significant degree of hearing loss. Additionally, apoptosis was immunohistologically examined with caspase-3 antibody in the cochlea. Caspase-3-positive cells (arrows in Figure 1B; n = 3) were observed in the spiral ganglion in the LPS infusion group, while no caspase-3-positive cells were observed in the control group (Figure 1B; n = 3). Moreover, TUNEL assay demonstrated apoptotic cochlear hair cells (arrow in Figure 1C; n = 3) and supporting cells (arrowheads in Figure 1C; n = 3) in the LPS group, while no TUNEL-positive cells were evident in the control group. These data suggest that LPS induced significant hearing loss accompanied by apoptosis in the cochlea.

Decreased levels of Hdac2, *Bcl-2*, and Bcl-xL in cochleae infused with LPS

To determine the expression pattern of Hdac2 after LPS infusion, we assessed Hdac2 transcript levels in cochleae from either LPS- or AP-infused guinea pigs by qRT-PCR. Consistent with our previous study,[5] significantly lower expression levels of Hdac2 were observed in cochleae from LPS-infused guinea pigs compared to the AP control group (unpaired Student's t test, **p < 0.01, n = 10; Figure 2A). To explore the relationship between Hdac2 and apoptosis-related genes, we also examined the expression levels of *Bcl-2* and Bcl-xL in cochlear mRNA pools. As illustrated in Figures 2B and 2C, the expression of *Bcl-2* and Bcl-xL was significantly decreased in cochleae of LPS-infused guinea pigs compared to AP controls (unpaired Student's t test, **p < 0.01, n = 10). Correlation analyses revealed that the levels of apoptosis-associated genes *Bcl-2* (Pearson correlation test, r = 0.751, p = 0.012, n = 10; Figure 2D) and Bcl-xL (Pearson correlation test, r = 0.713, p = 0.021, n = 10; Figure 2E) correlated positively with Hdac2 transcript levels, indicating the role of decreased Hdac2 levels in the downregulation of apoptosis-related genes in this animal model.

We also examined the relative protein levels of Hdac2 and several apoptosis-related genes in cochleae from these experimental cohorts by performing western blot analysis. Consistent with the qRT-PCR results, significantly lower protein levels of Bcl-xL, *Bcl-2*, and Hdac2 were detected in LPS-infused cochleae compared to AP-infused controls (unpaired Student's t test, **p < 0.01, n = 10; Figures 3A and 3B). However, the protein levels of pro-apoptosis genes, such as cleaved-caspase-3/9 and cleaved-PARP, were significantly increased in cochleae infused with LPS compared to AP-infused controls after normalizing to total caspase-3/9/PARP (unpaired Student's t test, **p < 0.01, n = 10; Figures 3A and 3C). These results indicate that Hdac2 might function as a regulator of apoptosis-related genes in the cochlea and participate in the apoptosis of hair cells and supporting cells.

Involvement of Hdac2 downregulation in hypoxia- or LPS-induced apoptosis of HEI-OC1 cells

To further investigate the expression of Hdac2 in cochlear cells *in vitro*, we cultured HEI-OC1 cells under hypoxic conditions and assessed the expression level of Hdac2 in response to hypoxia. As depicted in Figure 4, Hdac2 expression was dramatically decreased at both mRNA (Figure 4A) and protein (Figure 4B) levels when cells were exposed to hypoxia compared to normoxic controls (unpaired Student's t test, *p < 0.05, **p < 0.01, n = 3). The expression level

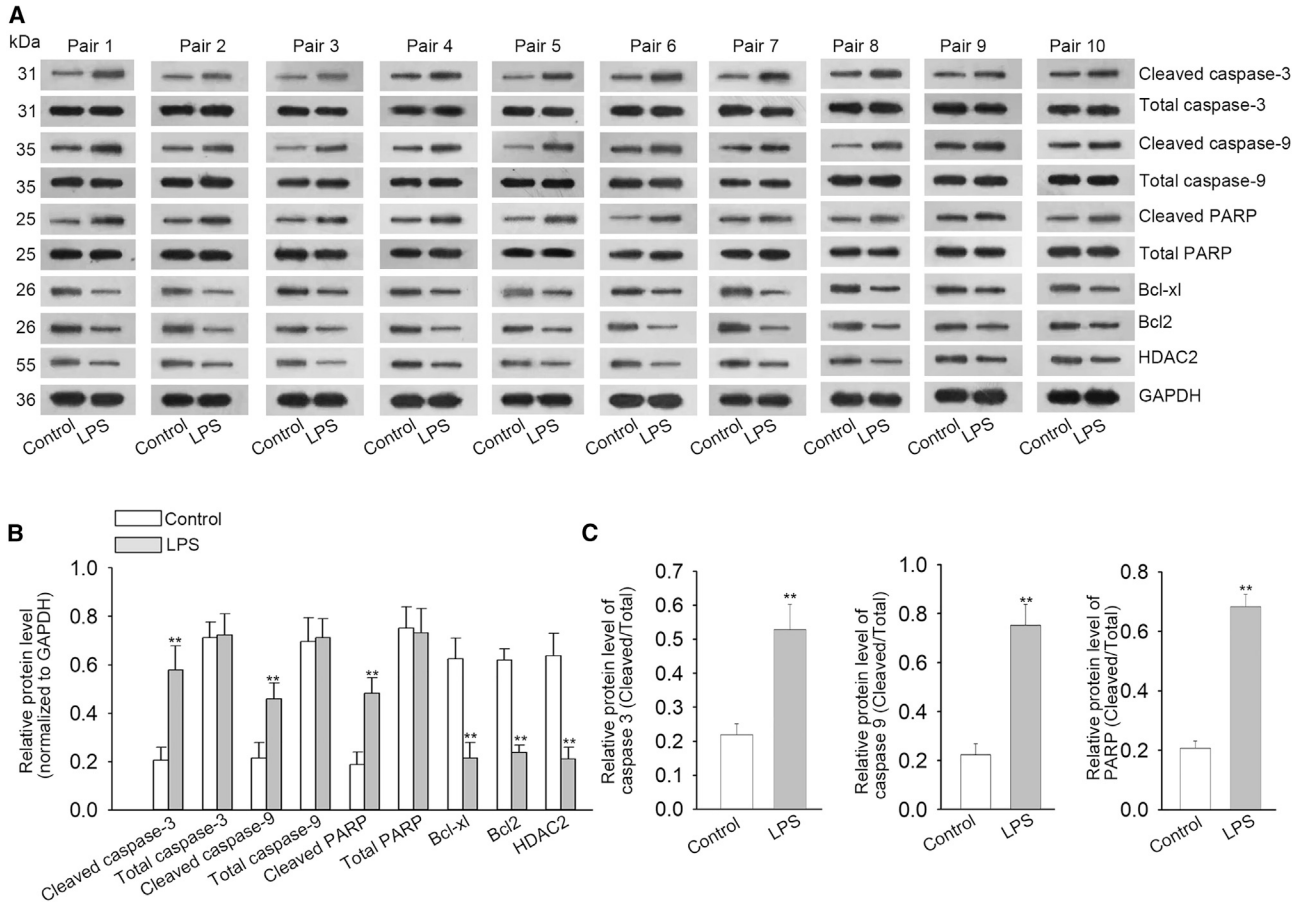

Figure 3. Decreased HDAC2 and Bcl-2 protein levels in LPS-infused cochleae

(A) Representative western blots of HDAC2 and apoptosis-related proteins (Bcl-2, Bcl-xL, cleaved-caspase 3/9/PARP, and total caspase 3/9/PARP) in the cochleae infused with LPS or AP (control). (B and C) Densitometric analyses of western blots indicate downregulated protein levels of HDAC2, Bcl-2, and Bcl-xL, and upregulated protein levels of cleaved-caspase 3/9/PARP (**$p < 0.01$). All data displayed as mean ± SD were obtained from three repeated and independent assays.

of Hdac2 was also decreased gradually in cells 6 to 24 h after LPS or hypoxia treatment (unpaired Student's t test, **$p < 0.01$, **$p < 0.01$, $n = 3$; Figures S1A and S1B). By using 3-(4,5-dimethylthiazol-2-yl)-2,5-diphenyltetrazolium bromide (MTT) assays, we evaluated the viability of HEI-OC1 cells with or without hypoxia treatment. As presented in Figure 4C, cells exposed to hypoxic conditions exhibited low viability 96 h after the treatment compared to non-hypoxic controls (two-way ANOVA, **$p < 0.01$, $n = 3$). Flow cytometry analyses revealed significantly more apoptotic cells in hypoxia-exposed cell populations compared to normoxic controls (unpaired Student's t test, **$p < 0.01$, $n = 3$; Figures 4D–4F). Similar findings were observed in HEI-OC1 cells exposed to LPS (unpaired Student's t test, **$p < 0.01$, $n = 3$; Figures S2A–S2C). Additionally, qRT-PCR analyses demonstrated that the expression levels of *Bcl-2* (unpaired Student's t test, **$p < 0.01$, $n = 3$; Figure 4G) and Bcl-xL (unpaired Student's t test, **$p < 0.01$, $n = 3$; Figure 4H) were significantly decreased in HEI-OC1 cells cultured under hypoxic conditions. Hypoxia-induced apoptosis was further demonstrated by trypan blue staining and TUNEL assay (unpaired Student's t test, **$p < 0.01$, $n = 3$; Figures 4I and 4J). Importantly, the mRNA and protein levels of Hdac2 were examined in HEI-OC1 cells treated with or without LPS. Consistent with our *in vivo* results, both mRNA and protein levels of Hdac2 were decreased in response to LPS treatment (unpaired Student's t test, **$p < 0.01$, $n = 3$; Figures S3A and S3B). By using western blot analysis, we confirmed that the levels of Bcl-xl, Bcl2, and Hdac2 were decreased in HEI-OC1 cells under hypoxic conditions (unpaired Student's t test, **$p < 0.01$, $n = 3$; Figures 5A–5C). In contrast, the relative protein levels of cleaved-caspase 3/9 and cleaved-PARP were significantly increased in HEI-OC1 cells cultured under hypoxic conditions (unpaired Student's t test, **$p < 0.01$, $n = 3$; Figures 5A–5C). Taken together, these results demonstrate that the downregulation of Hdac2 is involved in hypoxia-induced apoptosis *in vitro*.

To further investigate whether overexpression of Hdac2 could rescue cochlear cells from apoptosis induced by hypoxia *in vitro*, we transfected HEI-OC1 cells with Hdac2 overexpression

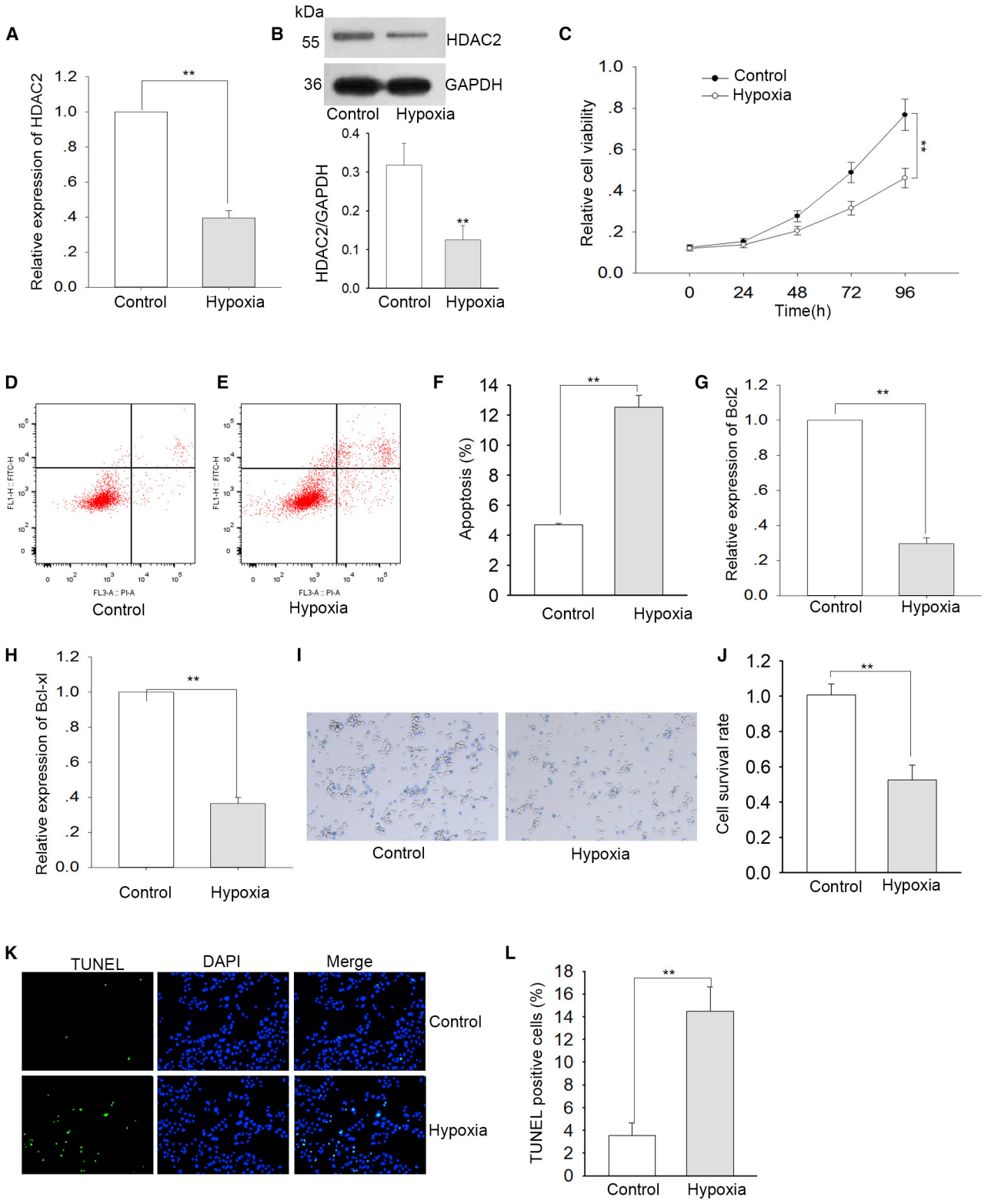

(legend on next page)

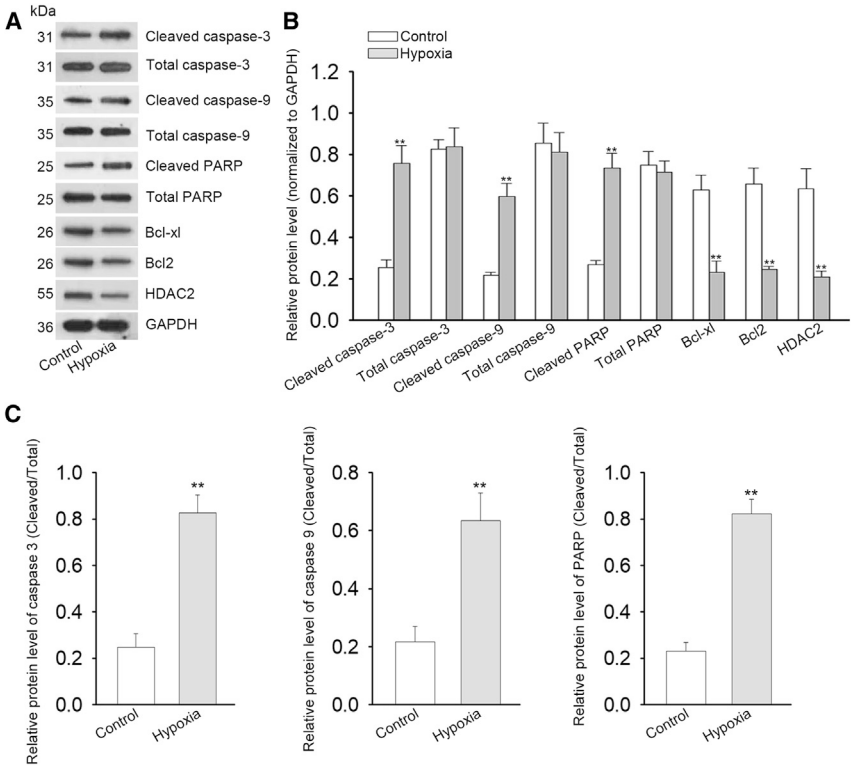

Figure 5. Decreased protein levels of HDAC2 and Bcl-2 in cells exposed to hypoxia

(A) Western blot evaluations of Bcl-2, Bcl-xL, HDAC2, cleaved-caspase 3/9, and cleaved-PARP in HEI-OC1 cells exposed to hypoxic or normoxic (control) culture conditions. (B and C) Densitometric analyses of western blots indicated hypoxia-induced significantly increased levels of apoptosis-related proteins and HDAC2 in HEI-OC1 cells (**p < 0.01). All data displayed as mean ± SD were obtained from three repeated and independent assays.

pcDNA3.1 under hypoxic conditions. As depicted in Figure S4A, Hdac2 overexpression was confirmed at both mRNA and protein levels in cells exposed to hypoxia compared to normoxic controls (one-way ANOVA, **p < 0.01, n = 3). By using MTT assays, we evaluated the viability of HEI-OC1 cells with hypoxia treatment in the Hdac2 overexpression group. As presented in Figure S4B, cells in the Hdac2 overexpression group exhibited higher viability 48–96 h after hypoxia compared to corresponding controls (one-way ANOVA, *p < 0.05, **p < 0.01, n = 3). Flow cytometry analyses revealed significantly fewer apoptotic cells in the Hdac2 overexpression group compared to corresponding controls (one-way ANOVA, **p < 0.01, n = 3; Figure S4C). Such reduced apoptosis in the Hdac2 overexpression group was further demonstrated by TUNEL assay (one-way ANOVA, **p < 0.01, n = 3; Figure S4D). Additionally, significantly increased levels of anti-apoptosis protein *Bcl-2* and significantly lower pro-apoptosis proteins, such as cleaved-caspase-3 and bax, were detected in the Hdac2 overexpression group compared to corresponding controls (one-way ANOVA, ** p < 0.01, n = 3; Figure S4E).

In the same way, we investigated whether the overexpression of Hdac2 could rescue cochlear cells from apoptosis induced by LPS. As depicted in Figure S5, Hdac2 overexpression was first confirmed at both mRNA and protein levels in cells treated with LPS compared to normoxic controls (one-way ANOVA, **p < 0.01, n = 3; Figure S5A). In this experiment, very similar results found in cells exposed to hypoxia were also observed in cells exposed to LPS in cell viability (one-way ANOVA, **p < 0.01, n = 3; Figure S5B), in apoptosis rate (one-way ANOVA, **p < 0.01, n = 3; Figure S5C), in TUNEL assay (one-way ANOVA, **p < 0.01, n = 3; Figure S5D), as well as in protein levels of *Bcl-2*, cleaved-caspase-3, and bax (one-way ANOVA, n = 3; Figure S5E).

Taken together, these results demonstrate that the downregulation of Hdac2 is involved in hypoxia- or LPS-induced apoptosis *in vitro*.

Hdac2 regulated *Bcl-2* through *miR-204-5p*

It has been documented that *Bcl-2* is subject to post-transcriptional regulation by miRNAs.[44–47] Hdac2 has been discovered to regulate apoptosis through miRNAs in cancers and bowel diseases.[33,34,48] Based on the results of positive correlation between Hdac2 and Bcl2, we hypothesized that miRNAs may be also involved in the downregulation of Hdac2 and BcL2. To examine this hypothesis, the potential binding miRNAs with *Bcl-2* were predicted by using online analysis tools, such as miRDB (http://www.mirdb.org/miRDB/), miRanda (http://www.microrna.org/), TargetScan (http://www.targetscan.org/), and PicTar (https://pictar.mdc-berlin.de/). We

Figure 4. Reduced HDAC2 expression and cell viability among HEI-OC1 cells cultured under hypoxic conditions

(A and B) The mRNA (A) and protein (B) levels of HDAC2 dramatically declined in HEI-OC1 cells exposed to hypoxia, compared with control cells (**p < 0.01). (C) Lower cell viability was estimated in cells under hypoxic conditions than those under normoxic control conditions (**p < 0.01). (D–F) Flow cytometry analysis of annexin-V in HEI-OC1 cells cultured under normoxic (control) or hypoxic conditions (**p < 0.01). (G and H) qRT-PCR detection also proved that the mRNA levels of Bcl-2 (G) and Bcl-xL (H) were overtly dropped in cells exposed to hypoxia (**p < 0.01). (I and J) Trypan blue staining showed the cell survival rate under conditions of normoxia or hypoxia (**p < 0.01). (K and L). TUNEL staining was applied to detect apoptosis ratio after treatment with normoxia or hypoxia (**p < 0.01). All data displayed as mean ± SD were obtained from three repeated and independent assays.

found that *miR-204-5p* and miR-211-5p were potential candidates for Hdac2-mediated *Bcl-2* regulation in several overlapping miRNAs through use of a Venn diagram (unpaired Student's t test, $^{**}p < 0.01$, n = 3; Figure 6A). We then assessed the levels of these two miRNAs in response to small interfering RNA (siRNA)-mediated Hdac2 silencing. As depicted in Figure 6B, the level of *miR-204-5p* was dramatically increased in HEI-OC1 cells transfected with a si-Hdac2 (unpaired Student's t test; NS, no significance; n = 3), indicating that *miR-204-5p* could be negatively regulated by Hdac2. To investigate *miR-204-5p* expression *in vivo*, we measured the *miR-204-5p* level in ten pairs of cochleae from the LPS- and AP-infusion cohorts. The *miR-204-5p* level was significantly increased in cochleae derived from LPS-treated guinea pigs compared to AP controls (unpaired Student's t test, $^{**}p < 0.01$, n = 3; Figure 6C), suggesting that *miR-204-5p* was also related to acute hearing loss induced by LPS infusion. To test the involvement of *miR-204-5p* in Hdac2-mediated *Bcl-2* regulation, we co-transfected HEI-OC1 cells with si-Hdac2 and a *miR-204-5p* inhibitor and then measured the mRNA and protein expression of *Bcl-2*. A dose response was observed in *miR-204-5p* levels when HEI-OC1 cells were cultured with different doses (20–100 nM) of *miR-204-5p* inhibitor. Approximately 100% of inhibition was observed when the concentration of *miR-204-5p* inhibitor reached 100 nM (unpaired Student's t test, $^{**}p < 0.01$, n = 3; Figure 6D). As depicted in Figure S6, *miR-204-5p* expression was dramatically increased in HEI-OC1 cells co-transfected with si-Hdac2 (one-way ANOVA, $^{**}p < 0.01$, n = 3). However, the increased expression of *miR-204-5p* was partially reversed by *miR-204-5p* inhibitor (one-way ANOVA, $^{**}p < 0.01$, n = 3). As revealed in Figures 6E–6G, the downregulation of *Bcl-2* induced by si-Hdac2 transfection could be reversed by *miR-204-5p* inhibitor (one-way ANOVA, $^{*}p < 0.05$, $^{**}p < 0.01$, n = 3), indicating that *miR-204-5p* is involved in Hdac2-mediated *Bcl-2* regulation. No changes were observed in miR-211-5p level in HEI-OC1 cells transfected with si-Hdac2 (Figure 6B; NS, no significance; n = 3).

Silencing Hdac2 enhances *miR-204-5p* expression through increasing the binding of Sp1 to miR-204 promoter

To better understand potential mechanisms of Hdac2 regulating *miR-204-5p*, we performed a sequence analysis on MIR204, the host gene of *miR-204-5p*. By applying the online transcription factor (TF) prediction software JASPAR (http://jaspar.genereg.net/), we found multiple Sp1 binding sites in MIR204 promoter regions, indicating that Sp1 might be a crucial transcription factor for *miR-204-5p*. Schematics of MIR204 promoters and potential and mutated Sp1-binding sites (Mut1-1-GTTCAGG-GGGCGGG-luciferase, Mut1-2-GGGCGGG-GTTCAGG-luciferase, Mut1-1/2-GTTCAGG-GTTCAGG-luciferase, Mut2-GTTCAGG-luciferase) are shown in Figure 7A.

The location of the binding sites at 1886 to 1895, 1752 to 1761, and 1685 to 1694 upstream of the transcription start site (TSS). To examine which site is the action one, we cloned them separately into pGL3 firefly luciferase reporters in luciferase reporter assays (sites 1 and 2 were used as p1 co-cloning vector and site 3 as p2 single cloning vector). Instead of cloning the whole promoter, we cloned each fragment that contains a site only.

Luminescence measurements demonstrated that the two promoters were infected and activated in HEI-OC1 cells (one-way ANOVA, $^{**}p < 0.01$, n = 3; Figure 7B), indicating successful synthesis of two promoter constructs.

To reveal the effect of Hdac2 downregulation on MIR204, si-Hdac2 was transfected into these reporter-infected HEI-OC1 cells and relative luciferase activities were measured. We found that Hdac2 silencing significantly increased the luciferase activity of two MIR204 luciferase promoter constructs (one-way ANOVA, si-Hdac2 compared to scrambled siRNA (scRNA)-transfected controls, $^{**}p < 0.01$, n = 3), while the effects of Hdac2 silencing on MIR-204-promoter-driven luciferase activity were decreased when the Sp1-binding sites were mutated (one-way ANOVA, ** or $^{\#\#}p < 0.01$, n = 3; Figure 7C). Furthermore, the upregulation of *miR-204-5p* induced by Hdac2 knockdown could be partially reversed by si-Sp1 when cells were co-transfected with si-Hdac2 and si-Sp1 (one-way ANOVA, $^{*}p < 0.05$, $^{**}p < 0.01$, n = 3; Figure 7D), indicating interaction between Hdac2 and Sp1. To confirm the interaction between Hdac2 and Sp1, we employed reciprocal co-immunoprecipitation (coIP) analyses with affinity-purified antibodies against Sp1 and Hdac2, and both targeting approaches resulted in co-immunoprecipitation of Hdac2 and Sp1 (Figures 7E and 7F; n = 3).

Additionally, results from chromatin IP (ChIP) assays demonstrated a co-localization of Hdac2 and Sp1 binding sites (one-way ANOVA, $^{**}p < 0.01$, n = 3; Figures 7G and 7H). Furthermore, it has been known that Hdac2 regulates gene expression via deacetylating core histones, so we explored whether Hdac2 could affect the *miR-204-5p* level by regulating acetylation of MIR204 promoter. The ChIP assay showed that silencing Hdac2 enhanced the histone-H3 acetylation level of MIR204 promoters specifically at Sp1-binding sites (one-way ANOVA, $^{**}p < 0.01$, n = 3; Figure 7I) and that silencing Hdac2 enhanced the SP1 level of MIR204 promoters (one-way ANOVA, $^{**}p < 0.01$, n = 3; Figure 7J), indicating that Hdac2 could affect Sp1 interaction with MIR204 by regulating the acetylation level of MIR204 promoter to regulate the *miR-204-5p* level. These observations demonstrated that Hdac2 could negatively regulate *miR-204-5p* expression through increasing the binding of Sp1 to *miR-204-5p* promoter.

A *miR-204-5p*/*Bcl-2*-dependent manner in apoptosis of HEI-OC1 cells induced by the downregulation of Hdac2

To further examine the influence of *miR-204-5p* and *Bcl-2* on apoptosis, HEI-OC1 cells were co-transfected with si-Hdac2 and *miR-204-5p* inhibitor or siHdac2 and a *Bcl-2* expression vector. As illustrated in Figure 8A, the decreased cell viability of HEI-OC1 cells resulting from Hdac2 silencing was partially reversed by inhibition of *miR-204-5p* or overexpression of *Bcl-2* (one-way ANOVA, $^{*}p < 0.05$, $^{**}p < 0.01$, n = 3; Figure 8A). Consistent with these results, the

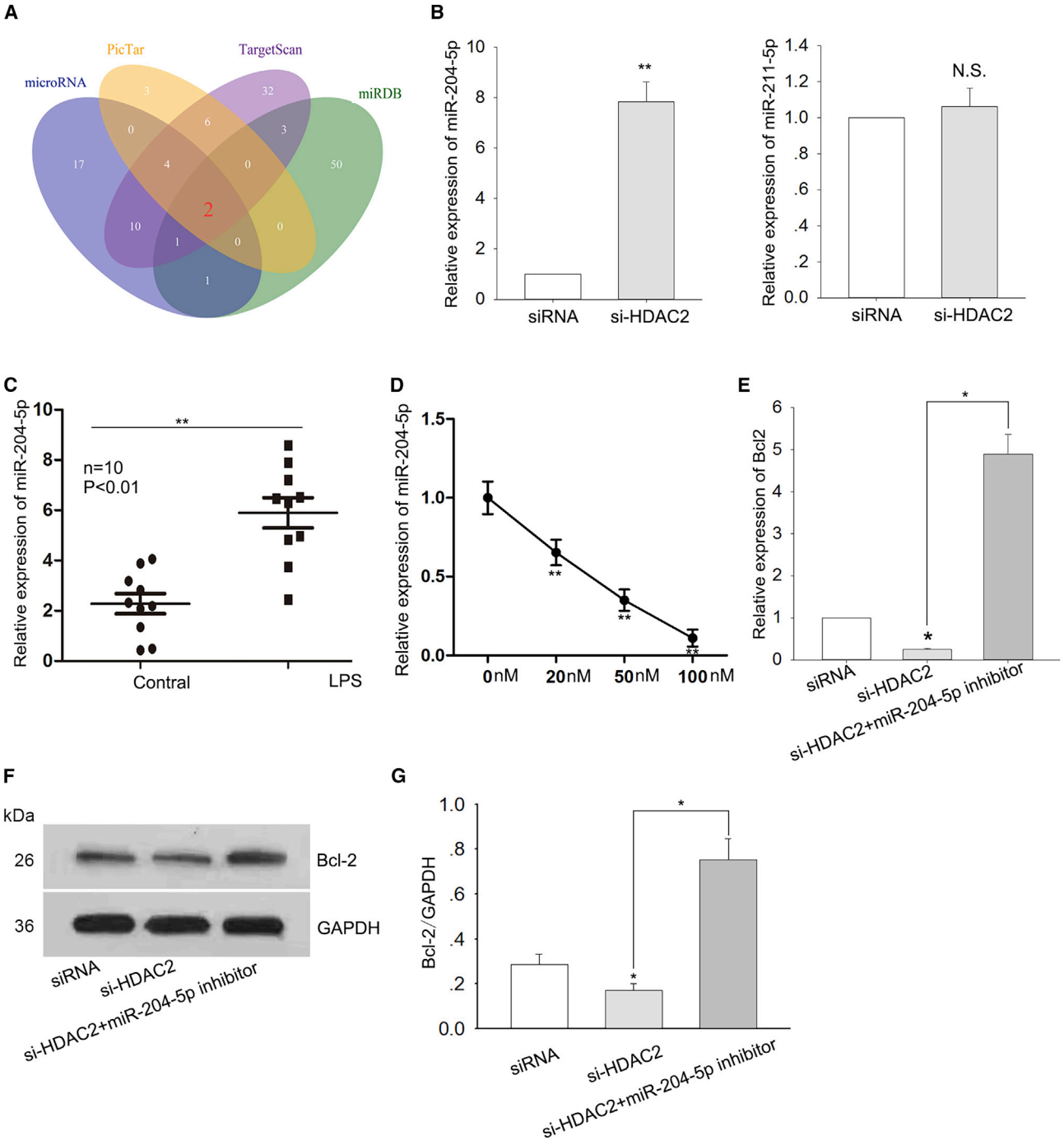

Figure 6. HDAC2 interacted with miR-204-5p to regulate Bcl-2 expression

(A) Overlapping miRNAs potentially binding to Bcl-2 transcripts were predicted by Venn diagram. Two miRNAs, miR-204-5p and miR-211-5p, were predicted to participate in HDAC2-mediated regulation of Bcl-2 expression. (B) The level of miR-204-5p increased in HEI-OC1 cells transfected with si-HDAC2 (**$p < 0.01$), while the mRNA of miR-211-5p was not significantly changed (N.S. indicates not significant). (C) The level of miR-204-5p was significantly increased in the cochleae derived from LPS-treated guinea pigs compared to controls (**$p < 0.01$). (D) Dose response in miR-204-5p levels was observed in HEI-OC1 cells cultured with different doses of miR-204-5p inhibitor. (E) Introduction of a miR-204-5p inhibitor reversed the downregulation of the Bcl-2 mRNA level in HEI-OC1 cells transfected with si-HDAC2 (**$p < 0.01$). (F) An example of western blot for relative Bcl-2 expression in HEI-OC1 cells treated with si-HDAC2 alone or si-HDAC2 plus miR-204-5p inhibitor. Representative images of western blot analysis of BcL2 expression in HEI-OC1 cells. (G) Densitometric analyses of western blot indicated a significant upregulation of Bcl-2 protein in HEI-OC1 cells co-transfected with si-HDAC2 and miR-204-5p inhibitor (*$p < 0.05$, **$p < 0.01$). All data displayed as mean ± SD were obtained from three repeated and independent assays.

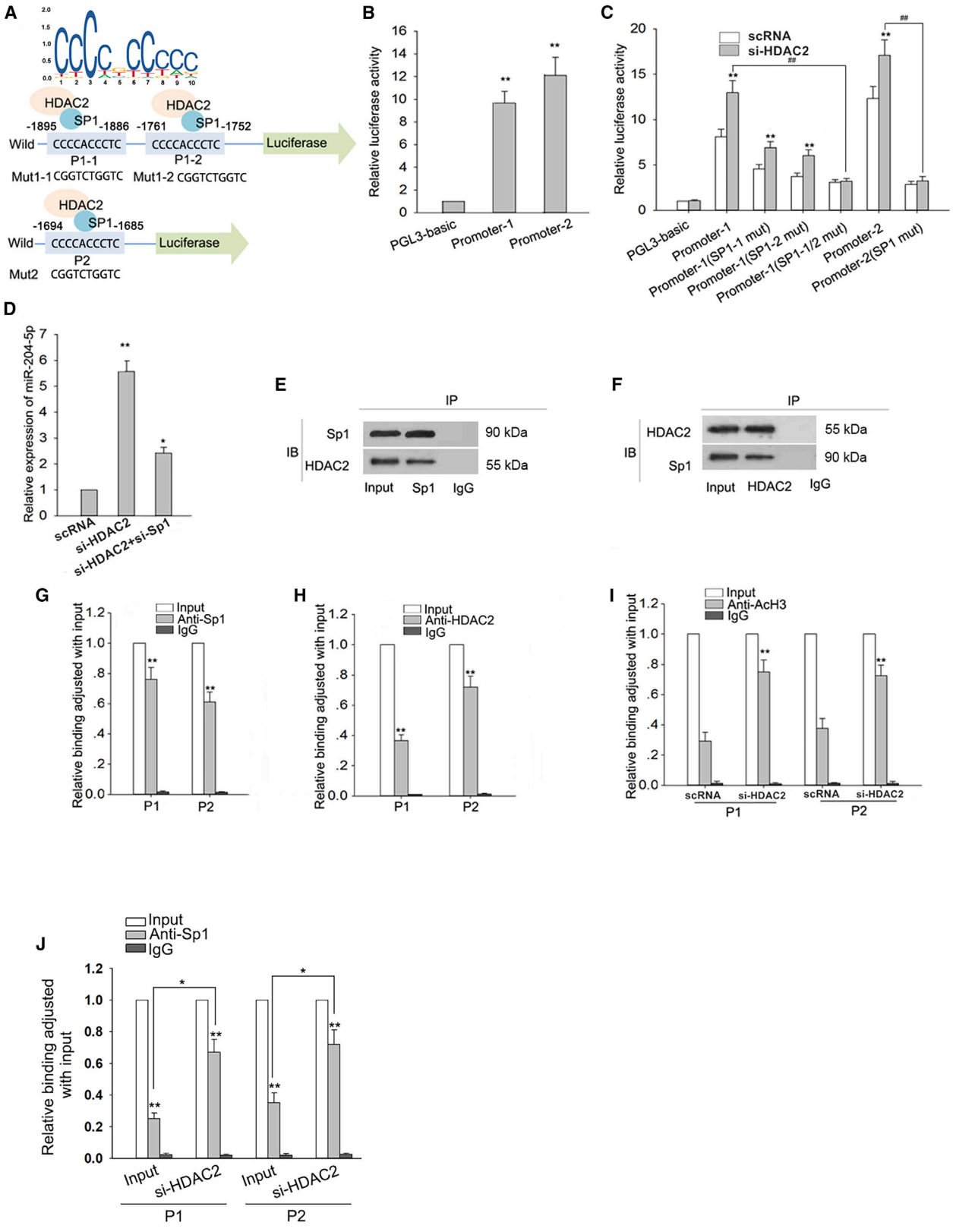

(legend on next page)

increased incidence of apoptosis resulting from Hdac2 inhibition could be partially mitigated by either co-transfection with the *miR-204-5p* inhibitor or the *Bcl-2* expression vector (one-way ANOVA, *p < 0.05, **p < 0.01, n = 3; Figures 8B and 8C). The cell survival rate was reduced after silencing Hdac2 but partially recovered in response to the knockdown of *miR-204-5p* or *Bcl-2* overexpression, and cell survival recovered to normal levels (scRNA control) after co-treatment with both *miR-204-5p* inhibitor and *Bcl-2* under Hdac2 depletion (one-way ANOVA, *p < 0.05, **p < 0.01, n = 3; Figures 8D and 8E). Consistent with these results, we observed similar effects of Hdac2 on apoptosis in TUNEL assay (one-way ANOVA, *p < 0.05, **p < 0.01, n = 3; Figures 8F and 8G). To examine whether overexpression of miR-204-5P could rescue cochlear cells from apoptosis, we evaluated the viability of HEI-OC1 cells co-transfected with Hdac2 overexpression and *miR-204-5p* mimic by using MTT assays. As depicted in Figure S8, cells co-transfected with Hdac2 overexpression exhibited higher viability 48–96 h after treatment (one-way ANOVA, *p < 0.05, **p < 0.01, n = 3). However, the increased cell viability of HEI-OC1 cells resulting from Hdac2 overexpression was partially reversed by *miR-204-5p* mimic (one-way ANOVA, **p < 0.01, n = 3; Figure S7). We also investigated whether inhibiting *miR-204-5p* could rescue HEI-OC1 cells from apoptosis induced by LPS (Figure S8). As presented in Figure S8A, cells treated with *miR-204-5p* inhibitor exhibited higher viability 48–96 h after treatment compared to corresponding controls (one-way ANOVA, **p < 0.01, n = 3). Flow cytometry analyses revealed significantly fewer apoptotic cells in the *miR-204-5p* inhibition group compared to corresponding controls (one-way ANOVA, **p < 0.01, n = 3; Figure S8B). Such reduced apoptosis was further demonstrated by TUNEL assay (one-way ANOVA, **p < 0.01, n = 3; Figure S8C). Additionally, significantly increased protein levels of anti-apoptosis protein *Bcl-2* and significantly lower pro-apoptosis proteins, such as cleaved-caspase-3 and bax, were detected in the *miR-204-5p* inhibition group compared to corresponding controls (one-way ANOVA, p < 0.01, n = 3; Figure S8D)

These observations support a conclusion that the downregulation of Hdac2 in HEI-OC1 cells was associated with pro-apoptotic programming, which was, at least in part, propagated through the *miR-204-5p*/*Bcl-2* axis.

DISCUSSION

In the present study, we provide insights into the manner of Hdac2-mediated regulation of apoptosis in an animal model of acute LPS-induced hearing loss and in HEI-OC1 cells cultured under hypoxic conditions or exposed to LPS. HDACs are chromatin-modulating enzymes that function to remove acetyl moieties from lysines in histone tails to inactivate genes, while histone acetyltransferases (HATs) function to add acetyl moieties to histone to activate genes.[49–51] Therefore, these two enzymes function antagonistically to epigenetically regulate target gene expression.[52] In *in vivo* experiments, we observed significant downregulation of Hdac2 in cochleae infused with LPS. Based on an immunohistochemical study in our previous study, Hdac2 is extensively distributed in the cochlea. Hdac2-positive cells include hair cells, supporting cells, spiral ganglion neurons, and cells in the stria vascularis. However, the downregulation of Hdac2 was not specific to any type of cells in the cochlea, although its overall expression was downregulated after LPS infusion.[5] The downregulation of HDACs was also observed in the aged mouse inner ear and in cardiac fibroblasts exposed to LPS,[53,54] as well as in SSNHL patients.[6–8] However, these observations are contradictory to previous reports of increased HDACs levels in the cochlea of noise- or ototoxic drug-exposed animals, or in the retina of ischemic injury.[55–57] It seems that different mechanisms are involved in the regulation of HDACs in the cochlea. LPS induced inflammation by activating HIF1 and hypoxia pathway gene responses in the testis,[58,59] as well as apoptosis by both intrinsic and extrinsic pathways.[60–62] In our acute hearing loss model, LPS may induce oxidative stress, provoke inner ear cells to release inflammatory cytokines, and eventually reduce Hdac2 activity or level.[54] In the present study, we use the LPS animal model to further explore the specific mechanisms of Hdac2 in cochlear hair cell apoptosis. The current results demonstrate that the downregulation of cochlear Hdac2 expression correlated strongly with the downregulation of *Bcl-2* and Bcl-xL and correlated with the upregulation of Caspases 3 and 9. Considering that LPS could induce a hypoxia microenvironment and regulate hypoxia-related genes *in vivo*,[58,59] we designed the *in vitro* experiments in HEI-OC1 cells treated with LPS or hypoxia. These results were recapitulated in HEI-OC1 cells cultured under hypoxic conditions or exposed to LPS. These findings indicated that downregulation of Hdac2 might regulate cochlear cell apoptosis by inhibiting *Bcl-2* and Bcl-xL and

Figure 7. Silencing HDAC2 enhances miR-204-5p expression through increasing the binding of Sp1 to miR-204 promoter

(A) Schematic of MIR204 promoters, the host gene of miR-204-5p, potential and mutated Sp1-binding sites. (B) Two promoters of MIR204 were infected and activated in HEI-OC1 cells in luciferase reporter assays (**p < 0.01). (C) si-HDAC2 treatment significantly increased luciferase activities of two MIR204 promoters (promoter-1 and -2) compared to a scrambled siRNA control (scRNA; **p < 0.01), while it decreased the activities of MIR204 promoters when Sp1-binding sites were mutated (**p < 0.01 compare to scRNA control; ##p < 0.01 compared to wild-type Sp1-binding site). (D) The level of miR-204-5p was upregulated in HEI-OC1 cells transfected with si-HDAC2 (*p < 0.05, **p < 0.01). The upregulation of miR-204-5p was partially reversed by co-transfecting with si-HDAC2 and si-SP1 (*p < 0.05). (E and F) HDAC2 and Sp1 co-immunoprecipitation by using affinity-purified antibodies against Sp1 (E) and HDAC2 (F), respectively, in HEI-OC1 cells. Western blots revealed that the levels of HDAC2 Sp1 were decreased (input indicates no-antibody controls). (G and H) ChIP performance in HEI-OC1 cells with anti-Sp1 (G), anti-HDAC2 (H), or anti-IgG control. Co-localization of HDAC2 and Sp1 binding sites were observed. (I) ChIP assays with an anti-acetyl-histone-H3 (AcH3) antibody to test the histone-H3 acetylation level of the MIR204 promoters at specific Sp1-binding sites. AcH3 was increased in HEI-OC1 cells transfected with si-HDAC2 (P1 and P2 indicate promoter-1 and promoter-2; **p < 0.01). (J) ChIP assays with an anti-SP1 antibody to test SP1 level of MIR204 promoters at specific Sp1-binding sites. SP1 level was increased in HEI-OC1 cells transfected with si-HDAC2 (P1 and P2 indicate promoter-1 and promoter-2; *p < 0.05). All data displayed as mean ± SD were obtained from three repeated and independent assays.

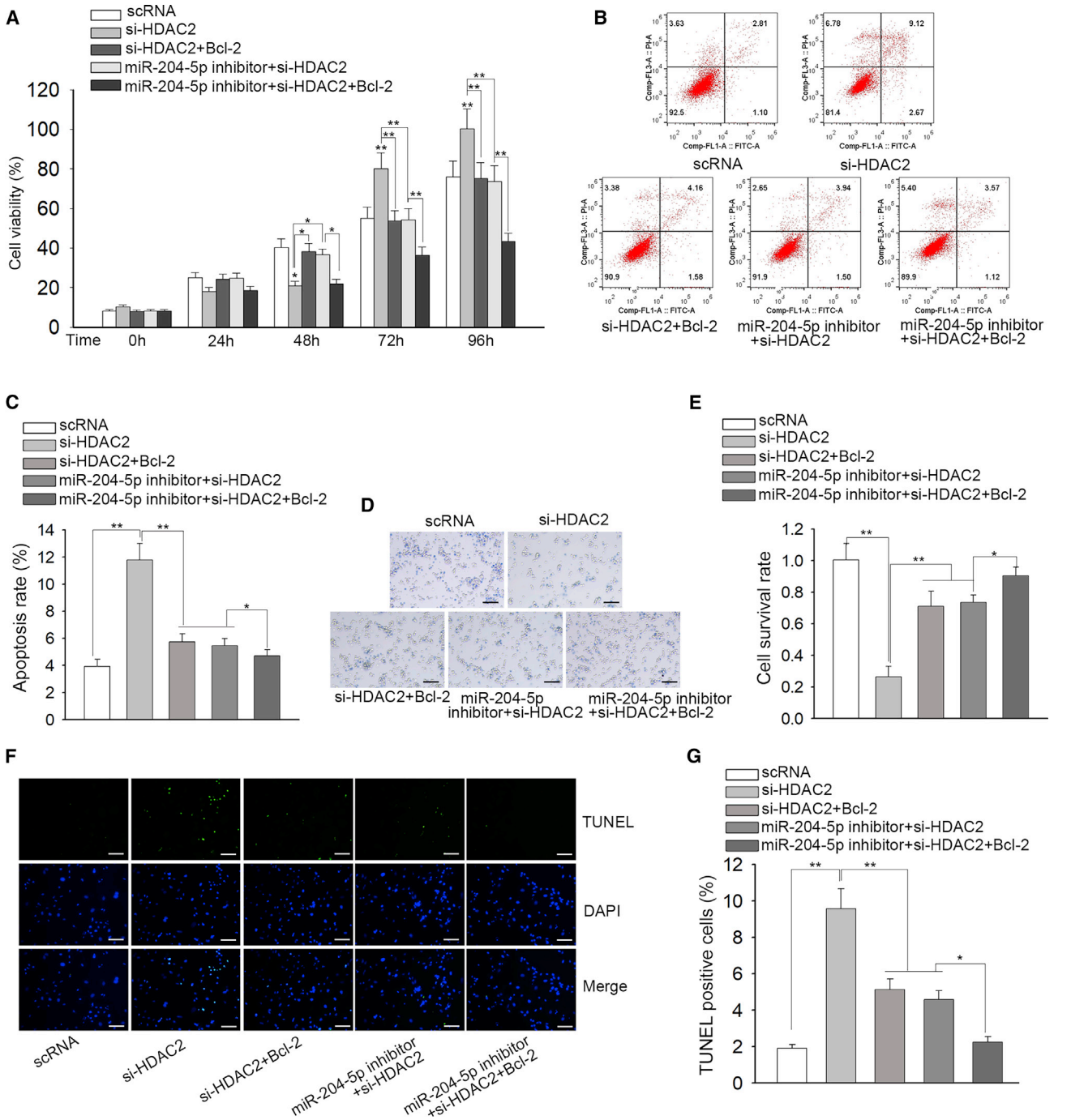

Figure 8. A miR-204-5p/Bcl-2-dependent manner in apoptosis of HEI-OC1 cells induced by the downregulation of HDAC2

Rescue assays were conducted in HEI-OC1 cells transfected with different plasmids: scRNA, si-HDAC2, si-HDAC2+miR-204-5p inhibitor, si-HDAC2+Bcl-2, si-HDAC2+miR-204-5p inhibitor+Bcl-2. (A) Cell viability was assessed in HEI-OC1 cells transfected with different plasmids. The decreased cell viability of HEI-OC1 cells resulting from HDAC2 silencing was partially reversed by inhibition of miR-204-5p or overexpression of Bcl-2 (*$p < 0.05$, **$p < 0.01$). (B) Flow cytometry analysis in HEI-OC cells transfected with indicated plasmids. (C) The increased incidence of apoptosis resulting from HDAC2 inhibition could be partially mitigated by either co-transfection with the miR-204-5p inhibitor or the Bcl-2 expression vector (*$p < 0.05$, **$p < 0.01$). (D) Representative images of trypan blue staining in HEI-OC1 cells transfected with different plasmids. (E) Reduced cell survival rate induced by HDAC2 knockdown was partially reversed by miR-204-5p knockdown or Bcl-2 overexpression.

(legend continued on next page)

activating Caspases 3 and 9. Therefore, it is reasonable to speculate that the upregulation of Hdac2 activity induced by glucocorticoids that was observed in our clinical studies[6–8] may inhibit apoptosis in the cochlea of SSNHL patients, although there is no direct evidence of involvement of apoptosis in SSNHL. However, this pathway or mechanism may not be able to apply to other SNHL animal models induced by ototoxic drugs or noise exposure, since increased HDAC levels were observed in those conditions.[55,56]

Recent studies have illustrated that inhibition of HDACs favors the activation of miRNAs, such as miR-15a, miR-29b, and miR-449.[52,63–65] miRNAs are a class of short RNAs (~21 nt) with no protein-coding ability that guides the post-transcriptional regulation of target genes. Some miRNAs have been documented to increase apoptosis of cochlear hair cells.[21,22] However, their roles in Hdac2-mediated *Bcl-2* regulation have not been elucidated. By Venn diagram of online analysis tools, *miR-204-5p* and miR-211-5p were potential regulatory miRNAs involved in Hdac2-mediated regulation of *Bcl-2* expression. The significant increase of miR-204-5p, but not miR-211-5p, in HEI-OC1 cells pre-treated with si-Hdac2 indicated that *miR-204-5p* is likely more sensitive to Hdac2-specific regulation in inner ear cells. This conclusion is supported by the apparent coordinated increase of *miR-204-5p* and decrease of Hdac2 and *Bcl-2* both in LPS-treated guinea pig cochleae and HEI-OC1 cells cultured under hypoxic conditions. It is also supported by the observation that *Bcl-2* downregulation induced by si-Hdac2 treatment could be reversed by co-transfection with an inhibitory nucleotide against *miR-204-5p*. A previous study demonstrated that *miR-204-5p* can directly target the 3′-UTR region of *Bcl-2* to induce preadipocyte apoptosis.[37,66] However, it is also possible that *miR-204-5p* may indirectly affect the level of Bcl2 by targeting the CRBA1 pathway.[67] Nevertheless, the detailed pathway outlined involving *miR-204-5p*, Sp1, and *Bcl-2* in the present study might be limited to the hypoxic model of HEI-OC1 cells and less to the *in vivo* guinea pig model.

To further explore the specific mechanism of Hdac2-mediated regulation of *miR-204-5p* expression, we analyzed MIR204, the host gene of *miR-204-5p*, and then identified several Sp1-binding sites in its promoter region. According to the literature, Sp1 can suppress the expression of miRNAs, suggesting it serves as a key transcriptional regulator of *miR-204-5p* expression.[68] We subsequently observed the decreased effect of si-Hdac2 on promoting MIR204 expression when Sp1-binding sites were mutated. Upregulated *miR-204-5p* levels induced by si-Hdac2 were partially reversed when si-Sp1 was introduced. These findings confirm our presumption that Sp1 plays a key role in Hdac2-mediated *miR-204-5p* expression. By a co-immunoprecipitation analysis and ChIP assays, we demonstrated that Hdac2 interacted with Sp1 at P1 and P2 sites, and the silencing of Hdac2 increased the histone-H3 acetylation level at these sites. By this mechanism, knockdown of Hdac2 could increase the activity of MIR204 promoters to regulate *miR-204-5p* expression in HEI-OC1 cells. In support of this paradigm, we observed an increase in relative cell viability and a decreased apoptosis in HEI-OC1 cells cultured under hypoxic conditions and co-transfected with si-Hdac2 and either a *miR-204-5p* inhibitor or a *Bcl-2* overexpression vector.

To our knowledge, this study presents, for the first time, a miRNA-related mechanism implicated in Hdac2-mediated processes associated with acute hearing loss. Our previous studies had suggested that a reduction of Hdac2 expression may correlate with poor prognosis and glucocorticoid resistance in SSNHL patients.[6,7] The present study suggests that *miR-204-5p* may vitally function in this pathological process and may, thus, represent a good therapeutic target to treat acute hearing loss. Inhibiting *miR-204-5p* may decrease apoptosis in the cochlea to improve the treatment effects of glucocorticoids in acute hearing loss, such as SSNHL patients with low Hdac2 expression. However, limitations still exist in our current study. For example, HEI-OC1 cells derived from the auditory organ of a transgenic mouse may not have the same characteristics as mature cochlear hair cells, although they express specific hair cell and supporting cell markers.[69] However, HEI-OC1 cells could represent common progenitors for cochlear sensory and supporting cells.[69,70] Thus, results from HEI-OC1 cells could provide useful information of hair-cell-related molecular pathways for further animal experiments. Although changes in Hdac2 levels in the model used in the present study are similar to our previous clinical studies in SSNHL,[6–8] the results we present here may not truly reflect the molecular mechanisms of SSNHL.

MATERIALS AND METHODS

Animals and cochlear LPS infusion

All procedures were performed under the guidance of the Medical Animal Care and Welfare Committee of Nanjing Drum Tower Hospital, Medical School of Nanjing University, China. A total of 32 albino guinea pigs (250 to 350 g) were randomly assigned into two groups (with or without LPS cochlear infusion, 16/group). All guinea pigs were screened with ABR, and only those with normal hearing were included in the present study. For cochlear infusion, guinea pigs were anesthetized with 10% chloral hydrate (0.5 mL/100 mg). The mastoid bulla was opened through a post-auricular incision, and a hole at the basal turn of cochlea was drilled under a surgical microscope. Five microliters of either AP alone (the control group) or 5 μL of AP containing 5 mg/mL of LPS (Sigma, USA; the LPS group) were infused into the cochlea. After cochlear infusion, the hole was sealed by using a small piece of muscle.[8]

Cell survival rate recovered to a normal level (scRNA control) after co-treatment with both miR-204-5p inhibitor and Bcl-2 under HDAC2 depletion (*$p < 0.05$, **$p < 0.01$). (F) Representative images of TUNEL staining in transfected HEI-OC1 cells. (G) Increased numbers of apoptotic cells induced by HDAC2 knockdown were reversed by co-transfection with miR-204-5p inhibitor and/or Bcl-2 (*$p < 0.05$, **$p < 0.01$). All data displayed as mean ± SD were obtained from three repeated and independent assays.

ABR

ABR thresholds were recorded in all guinea pigs 48 h after surgery. Animals were anesthetized with 10% chloral hydrate (0.5 mL/100 mg). The body temperature of guinea pigs was maintained at 38°C by an electric heating pad. The ABR signal was acquired through subcutaneous platinum needle electrodes at the vertex (active), the test ear (reference), and the contralateral ear pinna (ground). Response signals were amplified (100,000×), filtered, and procured via TDT Workstations (Tucker-Davis Technologies, USA). Fifteen millisecond tone bursts with a 1 ms rise/fall time were shown at a proportion of 10/s respectively at 4, 8, 16, and 32 kHz. Through reduction of the sound intensity at 5 dB intervals around the threshold, the average response to 1,000 stimuli was gained and defined as the critical value of stimulation decibel level with an evidently positive wave in the evoked response trace.

Cochlear epithelial cell harvesting

After the final ABR recording, ten guinea pigs from each group were euthanized with overdose of chloral hydrate (0.6 mL/100 mg), and temporal bones were removed quickly. The basilar membranes with the organs of Corti were dissected out in Hank's balanced salt solution (HBSS) under a dissecting microscope and soaked in HBSS with 0.5% trypsin for 15 min. The basilar membranes were then washed twice with 0.5 g/L bovine serum albumin in HBSS. After washing with HBSS, the basilar membranes were gently pipetted up and down to separate the sensory epithelial cells from the basilar membrane.[71] The cells were then rinsed with trypsin, collected, and stored at −20°C until further use.

Caspase-3 immunostaining

To examine apoptosis in AP- or LPS-infused cochleae, three guinea pigs from each group were randomly chosen after the final ABR recording. Animals were euthanized by overdose of chloral hydrate. The cochleae were gently perfused with pre-cold 4% paraformaldehyde (PFA) and fixed in the fixative overnight. After decalcification with 10% ethylenediaminetetraacetic acid (EDTA) and dehydration with ethanol, the cochleae were embedded with paraffin. Eight-micron mid-modiolar sections were collected and mounted on glass slides. Cochlear sections on selected slides were blocked with 5% normal goat serum in phosphate-buffered saline (PBS) for 1 h. After washing with PBS, the sections were incubated with an antibody against caspase-3 (1:100, #ab13847) overnight at 4°C. The sections were then incubated with a secondary antibody conjugated to horseradish peroxidase (HRP) for 1 h at 37°C. Immunostaining was visualized with the diaminobenzidine (DAB) Horseradish Peroxidase Color Development Kit (Beyotime Biotechnology, Shanghai, China). Nuclei were counterstained with hematoxylin. Immunostaining was examined with a light microscope.

TUNEL assay

To examine apoptosis in AP- or LPS-infused cochleae, three guinea pigs from each group were randomly chosen after the final ABR recording. Cochlear basilar membranes were dissected and subjected to the detection of TUNEL (Fluorescein *In Situ* Cell Death Detection Kit, Roche). Briefly, the basilar membranes were fixed in 4% paraformaldehyde for 1–2 h and then washed in PBS. For TUNEL detection, the basilar membranes were permeabilized with 20 μg/mL proteinase K for 5 min and then incubated in TUNEL reaction mix for 1 h at 37°C. The nuclei were counterstained with DAPI and observed under a confocal microscope.

Cell culture and transfection

HEI-OC1 cells were cultured with DMEM (Gibco, USA) along with 10% fetal bovine serum (FBS; JRH Biosciences, USA) and 50 U/mL interferon-γ at 37°C under 10% CO_2. After being cultured overnight under one of two different oxygen concentrations, 1% or 20%, cells were dissociated with trypsin and collected via centrifugation for subsequent experiments. In order to identify apoptotic pathways associated with Hdac2, HEI-OC1 cells were sequentially transfected with one of siRNAs (detailed below) using Lipofectamine 2000 (Invitrogen) or siRNA mate (Shanghai GenePharma Technology, Shanghai, China). HEI-OC1 cells (7×10^4) were seeded into six-well dishes before transfection. When the cells reached about 50% confluence, test nucleotides (scRNA, si-Hdac2, si-Sp1, *miR-204-5p* inhibitor [at a final concentration of 100 μM], and *Bcl-2* expression vector) and Lipofectamine 2000 (Invitrogen) were diluted to appropriate concentrations and combined in Opti-MEM medium according to the manufacture's protocol (Shanghai Shuangda Biotech, Shanghai, China). To optimize the *miR-204-5p* silencing effects, a dosage-response curve was generated. One hundred microliters of each transfection mixture was added into each well of HEI-OC1 cells. After incubation at 37°C under 5% CO_2 for 4–6 h, the cells were rinsed with fresh medium and then cultured with DMEM containing 10% FBS for another 18–48 h before harvesting with trypsin. The cells were collected and stored at −20°C until further use. The effect of transfection was verified by qRT-PCR and western blot (detailed below).

Quantitative real-time reverse transcription PCR

To assess the mRNA expression of Hdac2 and apoptotic genes in the cells extracted from guinea pig cochleae and HEI-OC1 cells, total RNA was extracted by using TRIzol reagent (Invitrogen; Thermo Fisher Scientific). Complementary DNA (cDNA) was generated by applying the EasyScript One-Step gDNA Removal and cDNA Synthesis SuperMix kit (Beijing Transgen Biotech, Beijing, China). Subsequently, qRT-PCR was used to determine the relative expression levels of Hdac2, *Bcl-2*, Bcl-xL, miR-211-5p, and *miR-204-5p* in the cochlea and HEI-OC1 cells. The primers used for qRT-PCR in the present study are listed in Table 1. Relative expression of each gene was normalized to an endogenous control, GAPDH, or U6 by the $2^{-\Delta\Delta CT}$ method.[72]

Cell viability

Relative HEI-OC1 cell viability was estimated by using the MTT assay kit (Sigma, USA) according to the manufacturer's protocol. Briefly, HEI-OC1 cells cultured in normoxic or hypoxic condition were treated with or without one of siRNAs, *miR-204-5p* inhibitor, or expression vectors for 24 h. After culturing with MTT for another 4 h, the cells were then harvested and centrifuged. After centrifuge,

Table 1. Primers used for mRNA expression of HDAC2 and apoptotic genes

Primers	Forward (5′-3′)	Reverse (5′-3′)
Si-HDAC2	ATACTTCCGAATTCAATAAGCA	GGTCGTGCCAATTACATTTCA
Bcl-2	TCATCCACATCCATCFFTTCAGCT	ATTCAATATTCAGTGTGTCTGT
Bcl-xL	ACCGGGAGTTAGTGATTGACT	ATCAAGTGGTCGGTCAAGTA
miR-211-5p	GGCTTCCCTTTGTCATCCT	TGCTCAGAGCCCATGGCG
miR-204-5p	TTCCCTTTGTCATCCTATGC	GCATAGGATGACAAAGGG
HDAC2	GACTATCGCCCCCACGTTT	GCTTCATGGGATGACCCTGT
GAPDH	CCTTGGACTTTGAGTCAAATT	GGTCGTGCCAATTACATTTCA
U6	CTCGCTTCGGCAGCACA	AACGCTTCACGAATTTGCGT

pellets were dissolved in 200 mL of dimethylsulfoxide. The relative amounts of the insoluble formazan product were then analyzed with optical density meter at a wavelength of 490 nm.

Flow cytometry analysis

The annexin-V fluorescein isothiocyanate (FITC)-propidium iodide (PI) Apoptosis kit (Invitrogen: Thermo Fisher Scientific) was used to assess apoptosis in HEI-OC1 cells. Before the analysis, HOEI-OC1 cells were transfected with one of the vectors and cultured for 48 h. The cells were then eluted with trypsin and washed twice with PBS. Approximately 2×10^5 cells were collected into each tube and suspended in 100 μL of binding buffer. After incubation with 5 μL of annexin V-FITC and 10 μL of PI staining solution for 10–15 min, the cells were then dissociated on ice in 400 μL of binding buffer. The samples were examined via flow cytometry within 1 h.

Western blots

To assess the protein expression of Hdac2 and apoptosis-related genes in cells extracted from either the cochleae of guinea pigs or HEI-OC1 cells, nuclear proteins were purified by using the Nuclear and Cytoplasmic Protein Extraction Kit (Beyotime Biotechnology, Shanghai, China). Protein concentration was estimated with the Bio-Rad Protein Assay Dye Reagent (Bio-Rad, CA, USA). One cochlea from each animal was used for protein extraction. Twenty-five micrograms of total protein lysates were then separated by sodium dodecyl sulfate-polyacrylamide gel electrophoresis (SDS-PAGE) and sequentially transferred onto polyvinylidene fluoride (PVDF) membranes (Millipore, USA). Following blocking in Tris Buffered saline Tween (TBST) with 5% skim milk for 2 h at 37°C, the membranes were incubated with one of the primary antibodies at 4°C for 8 h. The membranes were then washed with TBST three times and incubated with one of the appropriate HRP-conjugated secondary antibodies at 37°C for 2 h. The membranes were then washed five times with TBST and visualized by using a chemiluminescence kit (Thermo Fisher Scientific, Rockford, IL, USA). Antibodies used in the present study were purchased from Abcam (Hong Kong) and were used at the following dilutions: Hdac2 (1:1,000, #ab16032), *Bcl-2* (1:1,000, #ab32124), Bcl-xL (1:1,000, #ab32370), cleaved-caspase-3 (1:1,000, #ab2302), cleaved-caspase-9 (1:1,000, #ab2324), cleaved-PARP (1:1,000, #ab32064), and Sp1 (1:1,000, #ab13370). The antibody against GAPDH (1:5,000, #sc-25778) was purchased from Santa Cruz Biotechnology (USA).

Dual-luciferase reporter assay

To determine the influence of Hdac2 interactions with Sp1 on the promoter activity of *miR-204-5p*, HEI-OC1 cells were seeded into 96 wells (4×10^3 cells per well) and then co-transfected with one of the specific luciferase reporter plasmids, siRNAs, *miR-204-5p* inhibitor, or expression vectors, and Renilla-TK plasmid (Promega) transfection reagent. After incubation for 48 h, luciferase activities were examined with the Dual-Luciferase Reporter Assay kit (Promega, Madison, WI, USA) according to the manufacturer. Luciferase activities were normalized by *Renilla* luciferase activities. The data were expressed as fold changes relative to corresponding control group.

Co-immunoprecipitation assay

To determine whether Hdac2 interacts with Sp1, co-immunoprecipitation assays were performed by using the Co-immunoprecipitation Kit (Thermo Fisher Scientific, Rockford, IL, USA). One of the affinity-purified antibodies against Sp1 or Hdac2 (75 μg) was conjugated onto a spin column. Subsequently, cell lysates pre-cleared by control agarose resin were co-incubated with the resin column conjugated with an appropriate primary antibody at 4°C overnight. Bound proteins were eluted from the column at 4°C. Proteins in the eluant were separated by SDS-PAGE and then transferred to PVDF membranes. The relative amount of co-immunoprecipitated Hdac2 (for anti-Sp1-resin binding) or Sp1 (for anit-Hdac2 resin binding) was evaluated by western blot analyses as described above.

ChIP assays

ChIP assays were implemented by using the Immunoprecipitation Assay Kit (Millipore, Billerica, MA, USA). To cross-link histones to DNA, cells were incubated with 1% formaldehyde for 10 min at 37°C, resuspended in 200 μL of lysis buffer on ice for 10 min, and then sonicated by using Bioruptor 200 (Gene Channel Biotech,

Beijing, China). To shear crossed-linked DNA to 200 to 1,000 bp in length, the supernatant was pre-cleared with Salmon Sperm DNA/Protein A Agarose (50% slurry) to reduce non-specific background, then cultured with one of the primary antibodies against Sp1 (1:10, #ab13370), Hdac2 (1:5, #ab124974), acetyl-histone H3 (1:10, #ab4729), or IgG (1 ug/mL, #ab171870) overnight at 4°C with gentle rotation. Sequentially, the antibody/DNA complex was collected with Salmon Sperm DNA/Protein A Agarose for 1 h at 4°C with rotation in elution buffer. The crosslinks were reversed in 5 M NaCl at 65°C for 4 h. The purified DNA sample was measured with the assistance of qRT-PCR.

Statistical analysis

All of the data presented as the means ± standard deviation (SD) were analyzed with the software SPSS 17.0 (SPSS, Chicago, IL, USA). Multiple or two-group comparisons were analyzed with one-way or two-way ANOVA or Student's t test. Correlation between two factors was analyzed by Spearman's correlation analysis. p values <0.05 were considered significant.

SUPPLEMENTAL INFORMATION

Supplemental Information can be found online at https://doi.org/10.1016/j.omtn.2021.01.017.

ACKNOWLEDGMENTS

This study was supported by grants from the National Natural Science Funds of China (81670931), the Six Talent Peaks Project of Jiangsu Province, China (WSW-075), for clinical medicine from the Science and Technology Department of Jiangsu Province, China (BL 2014002), for the Key Project from the Science and Technology Department of Nanjing City, Jiangsu Province, China (ZKX17019), and Jiangsu Provincial Key Medical Discipline (ZDXKB2016015), China. The authors would like to thank Dr. Zachary Yokell in Hough Ear Institute for critically reviewing the manuscript.

AUTHOR CONTRIBUTIONS

W.S., L.X., and X.D. conceived experiments. L.X., Q.Z., X.C., Z.L., and B.F. performed experiments. L.X. and Q.Z. wrote the manuscript. W.S. and Y.D. secured funding. J.H. and Y.D. provided expertise. W.S. and X.D. reviewed manuscripts. W.S. and Y.D. supervised the research.

DECLARATION OF INTERESTS

The authors declare no competing interests.

REFERENCES

1. Gonneaud, A., Turgeon, N., Jones, C., Couture, C., Lévesque, D., Boisvert, F.M., Boudreau, F., and Asselin, C. (2019). HDAC1 and Hdac2 independently regulate common and specific intrinsic responses in murine enteroids. Sci. Rep. *9*, 5363.

2. Sun, D., Yu, M., Li, Y., Xing, H., Gao, Y., Huang, Z., Hao, W., Lu, K., Kong, C., Shimozato, O., et al. (2019). Histone deacetylase 2 is involved in DNA damage-mediated cell death of human osteosarcoma cells through stimulation of the ATM/p53 pathway. FEBS Open Bio *9*, 478–489.

3. Tang, W., Zhou, W., Xiang, L., Wu, X., Zhang, P., Wang, J., Liu, G., Zhang, W., Peng, Y., Huang, X., et al. (2019). The p300/YY1/miR-500a-5p/Hdac2 signalling axis regulates cell proliferation in human colorectal cancer. Nat. Commun. *10*, 663.

4. Tang, Y., Lin, Y.H., Ni, H.Y., Dong, J., Yuan, H.J., Zhang, Y., Liang, H.Y., Yao, M.C., Zhou, Q.G., Wu, H.Y., et al. (2017). Inhibiting Histone Deacetylase 2 (Hdac2) Promotes Functional Recovery From Stroke. J. Am. Heart Assoc. *6*, e007236.

5. Zhou, Q.Q., Dai, Y.H., Du, X.P., Hou, J., Qi, H., and She, W.D. (2017). Aminophylline restores glucocorticoid sensitivity in a guinea pig model of sudden sensorineural hearing loss induced by lipopolysaccharide. Sci. Rep. *7*, 2736.

6. Hou, J., She, W., Du, X., Dai, Y., Xie, L., and Zhou, Q. (2016). Histone Deacetylase 2 in Sudden Sensorineural Hearing Loss Patients in Response to Intratympanic Methylprednisolone Perfusion. Otolaryngol. Head Neck Surg. *154*, 164–170.

7. Zhang, X., Chen, J., Gao, Z., Qi, H., Dai, Y., and She, W. (2019). Response of Glucocorticoid Receptor Alpha and Histone Deacetylase 2 to Glucocorticoid Treatment Predicts the Prognosis of Sudden Sensorineural Hearing Loss. Clin. Exp. Otorhinolaryngol. *12*, 367–375.

8. Xie, L., Hou, J., Qi, H., Dai, Y., and She, W. (2019). Histone acetylation in refractory sudden sensorineural hearing loss patients after intratympanic methylprednisolone perfusion. J. Laryngol. Otol. *11*, 1–8.

9. Bodmer, D. (2017). An update on drug design strategies to prevent acquired sensorineural hearing loss. Expert Opin. Drug Discov. *12*, 1161–1167.

10. Kurabi, A., Keithley, E.M., Housley, G.D., Ryan, A.F., and Wong, A.C. (2017). Cellular mechanisms of noise-induced hearing loss. Hear. Res. *349*, 129–137.

11. Rybak, L.P., Mukherjea, D., and Ramkumar, V. (2019). Mechanisms of Cisplatin-Induced Ototoxicity and Prevention. Semin. Hear. *40*, 197–204.

12. Ozdamar, K., Sen, A., and Gonel, A. (2019). Assessment of Oxidative Stress in Patients with Sudden Hearing Loss: A Non-randomized Prospective Clinical Study. Indian J. Otolaryngol. Head Neck Surg. *71* (*Suppl 2*), 1543–1548.

13. Gul, F., Muderris, T., Yalciner, G., Sevil, E., Bercin, S., Ergin, M., Bababemez, M.A., and Kiris, M. (2017). A comprehensive study of oxidative stress in sudden hearing loss. Eur. Arch. Otorhinolaryngol. *274*, 1301–1308.

14. Nakagawa, T., Yamane, H., Takayama, M., Sunami, K., and Nakai, Y. (1998). Apoptosis of guinea pig cochlear hair cells following chronic aminoglycoside treatment. Eur. Arch. Otorhinolaryngol. *255*, 127–131.

15. Yang, W.P., Guo, W.W., Liu, H.Z., Xu, Y., Chen, L., and Hu, B.H. (2012). Age-related changes in the ratio of Mcl-1/Bax expression in the rat cochlea. Acta Otolaryngol. *132*, 123–132.

16. Chai, L., Gao, Y., Gu, Z.Y., and Ni, D.F. (2005). Apoptosis and apoptosis-related genes in experimental autoimmune inner ear disease. Zhonghua. Er. Bi. Yan. Hou. Tou. Jing. Wai. Ke. Za. Zhi *40*, 561–565.

17. Du, X., and Hamre, K.M. (2001). Increased cell death in the developing vestibulocochlear ganglion complex of the mouse after prenatal ethanol exposure. Teratology *64*, 301–310.

18. Esaki, S., Goshima, F., Kimura, H., Ikeda, S., Katsumi, S., Kabaya, K., Watanabe, N., Hashiba, M., Nishiyama, Y., and Murakami, S. (2011). Auditory and vestibular defects induced by experimental labyrinthitis following herpes simplex virus in mice. Acta Otolaryngol. *131*, 684–691.

19. Watanabe, K., Jinnouchi, K., Hess, A., Michel, O., and Yagi, T. (2001). Detection of apoptotic change in the lipopolysaccharide (LPS)-treated cochlea of guinea pigs. Hear. Res. *158*, 116–122.

20. Amarjargal, N., Andreeva, N., Gross, J., Haupt, H., Fuchs, J., Szczepek, A.J., and Mazurek, B. (2009). Differential vulnerability of outer and inner hair cells during and after oxygen-glucose deprivation in organotypic cultures of newborn rats. Physiol. Res. *58*, 895–902.

21. Tan, P.X., Du, S.S., Ren, C., Yao, Q.W., Zheng, R., Li, R., and Yuan, Y.W. (2014). MicroRNA-207 enhances radiation-induced apoptosis by directly targeting Akt3 in cochlea hair cells. Cell Death Dis. *5*, e1433.

22. Lin, Y., Shen, J., Li, D., Ming, J., Liu, X., Zhang, N., Lai, J., Shi, M., Ji, Q., and Xing, Y. (2017). MiR-34a contributes to diabetes-related cochlear hair cell apoptosis via SIRT1/HIF-1α signaling. Gen. Comp. Endocrinol. *246*, 63–70.

23. Bartel, D.P. (2004). MicroRNAs: genomics, biogenesis, mechanism, and function. Cell *116*, 281–297.

24. Larner-Svensson, H.M., Williams, A.E., Tsitsiou, E., Perry, M.M., Jiang, X., Chung, K.F., and Lindsay, M.A. (2010). Pharmacological studies of the mechanism and function of interleukin-1beta-induced miRNA-146a expression in primary human airway smooth muscle. Respir. Res. *11*, 68.

25. Nodine, M.D., and Bartel, D.P. (2010). MicroRNAs prevent precocious gene expression and enable pattern formation during plant embryogenesis. Genes Dev. *24*, 2678–2692.

26. Esteller, M. (2011). Non-coding RNAs in human disease. Nat. Rev. Genet. *12*, 861–874.

27. Hu, H., and Gatti, R.A. (2011). MicroRNAs: new players in the DNA damage response. J. Mol. Cell Biol. *3*, 151–158.

28. Mu, S., Kang, B., Zeng, W., Sun, Y., and Yang, F. (2016). MicroRNA-143-3p inhibits hyperplastic scar formation by targeting connective tissue growth factor CTGF/CCN2 via the Akt/mTOR pathway. Mol. Cell. Biochem. *416*, 99–108.

29. Oh, H.J., Kato, M., Deshpande, S., Zhang, E., Das, S., Lanting, L., Wang, M., and Natarajan, R. (2016). Inhibition of the processing of miR-25 by HIPK2-Phosphorylated-MeCP2 induces NOX4 in early diabetic nephropathy. Sci. Rep. *6*, 38789.

30. Wang, L., Wu, F., Song, Y., Li, X., Wu, Q., Duan, Y., and Jin, Z. (2016). Long noncoding RNA related to periodontitis interacts with miR-182 to upregulate osteogenic differentiation in periodontal mesenchymal stem cells of periodontitis patients. Cell Death Dis. *7*, e2327.

31. Xue, T., Wei, L., Zha, D.J., Qiu, J.H., Chen, F.Q., Qiao, L., and Qiu, Y. (2016). miR-29b overexpression induces cochlear hair cell apoptosis through the regulation of SIRT1/PGC-1α signaling: Implications for age-related hearing loss. Int. J. Mol. Med. *38*, 1387–1394.

32. Xiong, H., Pang, J., Yang, H., Dai, M., Liu, Y., Ou, Y., Huang, Q., Chen, S., Zhang, Z., Xu, Y., et al. (2015). Activation of miR-34a/SIRT1/p53 signaling contributes to cochlear hair cell apoptosis: implications for age-related hearing loss. Neurobiol. Aging *36*, 1692–1701.

33. Hsieh, T.H., Hsu, C.Y., Tsai, C.F., Long, C.Y., Wu, C.H., Wu, D.C., Lee, J.N., Chang, W.C., and Tsai, E.M. (2015). HDAC inhibitors target HDAC5, upregulate microRNA-125a-5p, and induce apoptosis in breast cancer cells. Mol. Ther. *23*, 656–666.

34. Srinivas, C., Swathi, V., Priyanka, C., Anjana Devi, T., Subba Reddy, B.V., Janaki Ramaiah, M., Bhadra, M., and Pal Bhadra, M. (2016). Novel SAHA analogues inhibit HDACs, induce apoptosis and modulate the expression of microRNAs in hepatocellular carcinoma. Apoptosis *21*, 1249–1264.

35. Li, M., Shen, Y.J., Wang, Q., and Zhou, X.F. (2019). MiR-204-5p promotes apoptosis and inhibits migration of osteosarcoma via targeting EBF2. Biochimie *158*, 224–232.

36. Fan, C.F., Liu, X.M., Li, W.F., Wang, H.Y., Teng, Y.L., Ren, J., and Huang, Y.S. (2019). Circular RNA circ KMT2E is up-regulated in diabetic cataract lenses and is associated with miR-204-5p sponge function. Gene *710*, 170–177.

37. Du, J.J., Zhang, P.W., Gan, M.L., Zhao, X., Xu, Y., Li, Q., Jiang, Y.Z., Tang, G.Q., Li, M.Z., Wang, J.Y., et al. (2018). MicroRNA-204-5p regulates 3T3-L1 preadipocyte proliferation, apoptosis and differentiation. Gene *668*, 1–7.

38. Sheng, L.J., Wu, J., Gong, X.W., Dong, D., and Sun, X.X. (2018). SP1-induced upregulation of lncRNA PANDAR predicts adverse phenotypes in retinoblastoma and regulates cell growth and apoptosis in vitro and in vivo. Gene *668*, 140–145.

39. Zhang, X., Zhuang, H., Han, F., Shao, X., Liu, Y., Ma, X., Wang, Z., Qiang, Z., and Li, Y. (2018). Sp1-regulated transcription of RasGRP1 promotes hepatocellular carcinoma (HCC) proliferation. Liver Int. *38*, 2006–2017.

40. Xu, Y., Yao, Y., Jiang, X., Zhong, X., Wang, Z., Li, C., Kang, P., Leng, K., Ji, D., Li, Z., et al. (2018). SP1-induced upregulation of lncRNA SPRY4-IT1 exerts oncogenic properties by scaffolding EZH2/LSD1/DNMT1 and sponging miR-101-3p in cholangiocarcinoma. J. Exp. Clin. Cancer Res. *37*, 81.

41. Aydemir, A.T., Meltem, A., and Feray, K. (2018). SP1-mediated downregulation of ADAMTS3 gene expression in osteosarcoma models. Gene *659*, 1–10.

42. Banerjee, A., Mahata, B., Dhir, A., Mandal, T.K., and Biswas, K. (2019). Elevated histone H3 acetylation and loss of the Sp1-HDAC1 complex de-repress the GM2-synthase gene in renal cell carcinoma. J. Biol. Chem. *294*, 1005–1018.

43. Guo, Y., Su, Z., Yang, W., and Jiang, S. (2001). Isolation of outer hair cells from varying turns of the guinea-pig cochlea. Lin. Chuang. Er. Bi. Yan. Hou. Ke. Za. Zhi *15*, 26–27.

44. Zhao, J., Ou, S.L., Wang, W.Y., Yan, C., and Chi, L.X. (2017). MicroRNA-1907 enhances atherosclerosis-associated endothelial cell apoptosis by suppressing Bcl-2. Am. J. Transl. Res *9*, 3433–3442.

45. Liu, Y., Yang, L., Yin, J., Su, D., Pan, Z., Li, P., and Wang, X. (2018). MicroRNA-15b deteriorates hypoxia/reoxygenation-induced cardiomyocyte apoptosis by downregulating Bcl-2 and MAPK3. J. Investig. Med. *66*, 39–45.

46. Kim, J.H., Lee, H., Shin, E.A., Kim, D.H., Choi, J.B., and Kim, S.H. (2017). Implications of Bcl-2 and its interplay with other molecules and signaling pathways in prostate cancer progression. Expert Opin. Ther. Targets *21*, 911–920.

47. Zhao, K., Zhang, Y., Kang, L., Song, Y., Wang, K., Li, S., Wu, X., Hua, W., Shao, Z., Yang, S., et al. (2017). Epigenetic silencing of miRNA-143 regulates apoptosis by targeting BCL2 in human intervertebral disc degeneration. Gene *628*, 259–266.

48. Felice, C., Lewis, A., Armuzzi, A., Lindsay, J.O., and Silver, A. (2015). Review article: selective histone deacetylase isoforms as potential therapeutic targets in inflammatory bowel diseases. Aliment. Pharmacol. Ther. *41*, 26–38.

49. Baek, S.H. (2011). When signaling kinases meet histones and histone modifiers in the nucleus. Mol. Cell *42*, 274–284.

50. Yamagoe, S., Kanno, T., Kanno, Y., Sasaki, S., Siegel, R.M., Lenardo, M.J., Humphrey, G., Wang, Y., Nakatani, Y., Howard, B.H., and Ozato, K. (2003). Interaction of histone acetylases and deacetylases in vivo. Mol. Cell. Biol. *23*, 1025–1033.

51. Wang, Z.B., Zang, C.Z., Cui, K.R., Schones, D.E., Barski, A., Peng, W.Q., and Zhao, K. (2009). Genome-wide mapping of HATs and HDACs reveals distinct functions in active and inactive genes. Cell *138*, 1019–1031.

52. Sampath, D., Liu, C.M., Vasan, K., Sulda, M., Puduvalli, V.K., Wierda, W.G., and Keating, M.J. (2012). Histone deacetylases mediate the silencing of miR-15a, miR-16, and miR-29b in chronic lymphocytic leukemia. Blood *119*, 1162–1172.

53. Takumida, M., Takumida, H., Katagiri, Y., and Anniko, M. (2016). Localization of sirtuins (SIRT1-7) in the aged mouse inner ear. Acta Otolaryngol. *136*, 120–131.

54. Zhang, H., He, Y., Zhang, G., Li, X., Yan, S., Hou, N., Xiao, Q., Huang, Y., Luo, M., Zhang, G., et al. (2017). Hdac2 is required by the physiological concentration of glucocorticoid to inhibit inflammation in cardiac fibroblasts. Can. J. Physiol. Pharmacol. *95*, 1030–1038.

55. Chen, J., Hill, K., and Sha, S.H. (2016). Inhibitors of Histone Deacetylases Attenuate Noise-Induced Hearing Loss. J. Assoc. Res. Otolaryngol. *17*, 289–302.

56. Fan, J., Alsarraf, O., Dahrouj, M., Platt, K.A., Chou, C.J., Rice, D.S., and Crosson, C.E. (2013). *I*nhibition of Hdac2 protects the retina from ischemic injury. Invest. Ophthalmol. Vis. Sci. *54*, 4072–4080.

57. Layman, W.S., Williams, D.M., Dearman, J.A., Sauceda, M.A., and Zuo, J. (2015). Histone deacetylase inhibition protects hearing against acute ototoxicity by activating the Nf-κB pathway. Cell Death Discov. *1*, 15012.

58. Yang, N., Liang, Y., Yang, P., and Ji, F. (2017). Propofol suppresses LPS-induced nuclear accumulation of HIF-1α and tumor aggressiveness in non-small cell lung cancer. Oncol. Rep. *37*, 2611–2619.

59. Palladino, M.A., Fasano, G.A., Patel, D., Dugan, C., and London, M. (2018). Effects of lipopolysaccharide-induced inflammation on hypoxia and inflammatory gene expression pathways of the rat testis. Basic Clin. Androl. *28*, 14.

60. Xu, J., Lin, C., Wang, T., Zhang, P., Liu, Z., and Lu, C. (2018). Ergosterol Attenuates LPS-Induced Myocardial Injury by Modulating Oxidative Stress and Apoptosis in Rats. Cell. Physiol. Biochem. *48*, 583–592.

61. Markotic, A., Flegar, D., Grcevic, D., Sucur, A., Lalic, H., Turcic, P., Kovacic, N., Lukac, N., Pravdic, D., Vukojevic, K., et al. (2020). LPS-induced inflammation desensitizes hepatocytes to Fas-induced apoptosis through Stat3 activation-The effect can be reversed by ruxolitinib. J. Cell. Mol. Med. *24*, 2981–2992.

62. Pan, P., Zhang, H.M., Su, L.X., Wang, X.T., and Liu, D.W. (2018). Melatonin Balance the Autophagy and Apoptosis by Regulating UCP2 in the LPS-Induced Cardiomyopathy. Molecules *23*, 675.

63. Lynch, S.M., O'Neill, K.M., McKenna, M.M., Walsh, C.P., and McKenna, D.J. (2016). Regulation of miR-200c and miR-141 by Methylation in Prostate Cancer. Prostate *76*, 1146–1159.

64. Adams, B.D., Parsons, C., Walker, L., Zhang, W.C., and Slack, F.J. (2017). Targeting noncoding RNAs in disease. J. Clin. Invest. *127*, 761–771.

65. Chen, L., Luo, L., Chen, W., Xu, H.X., Chen, F., Chen, L.Z., Zeng, W.T., Chen, J.S., and Huang, X.H. (2016). MicroRNA-24 increases hepatocellular carcinoma cell metastasis and invasion by targeting p53: miR-24 targeted p53. Biomed. Pharmacother. *84*, 1113–1118.

66. Lin, Y.C., Lin, J.F., Tsai, T.F., Chou, K.Y., Chen, H.E., and Hwang, T.I.S. (2017). Tumor suppressor miRNA-204-5p promotes apoptosis by targeting BCL2 in prostate cancer cells. Asian J. Surg. *40*, 396–406.

67. Bian, Z., Jin, L., Zhang, J., Yin, Y., Quan, C., Hu, Y., Feng, Y., Liu, H., Fei, B., Mao, Y., et al. (2016). LncRNA-UCA1 enhances cell proliferation and 5-fluorouracil resistance in colorectal cancer by inhibiting miR-204-5p. Sci. Rep. *6*, 23892.

68. Zhao, N., Li, S., Wang, R., Xiao, M., Meng, Y., Zeng, C., Fang, J.H., Yang, J., and Zhuang, S.M. (2016). Expression of microRNA-195 is transactivated by Sp1 but inhibited by histone deacetylase 3 in hepatocellular carcinoma cells. Biochim. Biophys. Acta *1859*, 933–942.

69. Kalinec, G.M., Webster, P., Lim, D.J., and Kalinec, F. (2003). A cochlear cell line as an in vitro system for drug ototoxicity screening. Audiol. Neurotol. *8*, 177–189.

70. Kalinec, G.M., Park, C., Thein, P., and Kalinec, F. (2016). Working with Auditory HEI-OC1 Cells. J. Vis. Exp. *115*, 54425.

71. Sobkowicz, H.M., Loftus, J.M., and Slapnick, S.M. (1993). Tissue culture of the organ of Corti. Acta Otolaryngol. Suppl. *502*, 3–36.

72. Livak, K.J., and Schmittgen, T.D. (2001). Analysis of relative gene expression data using real-time quantitative PCR and the 2(-Delta Delta C(T)) Method. Methods *25*, 402–408.